# NJC

Accepted Manuscript


This is an *Accepted Manuscript*, which has been through the Royal Society of Chemistry peer review process and has been accepted for publication.

*Accepted Manuscripts* are published online shortly after acceptance, before technical editing, formatting and proof reading. Using this free service, authors can make their results available to the community, in citable form, before we publish the edited article. We will replace this *Accepted Manuscript* with the edited and formatted *Advance Article* as soon as it is available.

You can find more information about *Accepted Manuscripts* in the Information for Authors.

Please note that technical editing may introduce minor changes to the text and/or graphics, which may alter content. The journal's standard Terms & Conditions and the Ethical guidelines still apply. In no event shall the Royal Society of Chemistry be held responsible for any errors or omissions in this *Accepted Manuscript* or any consequences arising from the use of any information it contains.

ROYAL SOCIETY OF CHEMISTRY

www.rsc.org/njc

# Mimicking vanadium haloperoxidases: vanadium(III)-carboxylic acid complexes and their application in $H_2O_2$ detection

Xiao Dong Feng[a], Xiao Xi Zhang[a], Zhi Nan Wang[a], Jian Song[a], Yong Heng Xing[a*] and Feng Ying Bai[b*]

**ABSTRACT:** Vanadium(III) complexes $[V(2,6\text{-pdc})_2(H_2O)_2]\cdot 2H_2O$ (**1**), $V(2,6\text{-pdc})(htba)(H_2O)_2$ (**2**), ( 2,6-pdc = 2,6-pyridinedicarboxylic acid, htba = 2-acetoxy-4-trifluoromethylbenzoic acid ) have been synthesized by the reaction of $V_2(SO_4)_3$, 2,6-pdc (for **1**), 2,6-pdc and htba (for **2**) under hydrothermal condition at 120 °C for 36 hours. Because the vanadium (III) was easy to be oxidized into higher oxidation State, we put reducing agents vitamin C to protect the center vanadium(III) to be oxidized. They were characterized by elemental analysis, IR, UV-vis, and the single-crystal X-ray diffraction analysis. Structural analysis reveals that centre metal V atom in the complexes **1** and **2** are seven-coordination mode, forming pentagonal bipyramid geometries with NO6 donors. The complexes catalyzed organic substrate phenol red in the presence of $H_2O_2$, bromide and buffer exhibiting catalytic bromination activity. Comparing with other oxidation state had better catalytic activity (the maximum reaction rate constant was $2.424\times10^2$ k(mol $L^{-1})^{-2}s^{-1}$). The mimicking vanadium haloperoxidases als**o** overcame some serious disadvantages of natural enzymes. Therefore, the reaction system can be considered as an effective model for hydrogen peroxide determination.

## Introduction

Hydrogen peroxide is an integral part of atmospheric chemistry and biological systems. In the atmosphere, it is an oxidant that is produced from the combination of hydroperoxyl radicals ($HO_2\cdot$) and their hydrated form[1]. Hydrogen peroxide is exceptionally soluble in water and it is thought to be the most efficient oxidant in the formation of $H_2SO_4$ from dissolved $SO_2$. This implies that hydrogen peroxide could have some effects in the acidity of rainwater[2]. Otherwise, hydrogen peroxide is of great practical importance in many fields such as food, pharmaceutical, clinical, industrial[3-6]. Hence, it is urgent in need to establish a convenient，effective and rapid method to detect $H_2O_2$.

Nowadays, there have been numerous detection methods for $H_2O_2$[7-14], colorimetric method is one of the most popular determination of $H_2O_2$, others including HPLC, electrochemistry detection, chemiluminescence, etc.[15-20]. Titanium-based assays (Ti-PAPS reagents) were developed in the 1980's for spectrophotometric detection of $H_2O_2$[9]. The Fox assay was developed in 1990's based on ferrous ion oxidation in the presence of the ferric ion indicator xylenol orange under acidic conditions [10]. Recently, Luo and co-workers developed a detection method based on oxidation of methyl orange using an iron-catalyzed Fenton reaction system under acidic conditions[12]. Other methods, such as fluorescent probes have recently been developed to monitor hydrogen peroxide production in living cells[13]. Chemiluminescence methods have also been developed recently[14]. These methods are highly sensitive, but they are limited by complicated apparatus setup and sensor preparation, interferences from metal ions. Based on the points above, we used colorimetric method to detect $H_2O_2$.

To our knowledge, vanadium haloperoxidases (V-HPOs) which are found in marine algae are able to accelerate the oxidative halogenation of organic compounds in the presence of hydrogen peroxide, organic hydroperoxides or molecular oxygen[21-23]. Unfortunately, natural enzymes are proteins and inherently bear some serious disadvantages, such as easy denaturation by environmental changes, digestion by proteases, as well as time-consuming and expensive preparation and purification, therefore, much effort has been put into developing stable artificial enzyme mimics of vanadium complexes as a functional model for V-HPOs[24-28].

Vanadium complexes are able to mimic a reaction in which vanadium catalyzed the bromination of organic substrates in the presence of $H_2O_2$ and bromide[26-31]. Through the experiment results, it is found that the oxidation reaction catalyzed by the vanadium complexes is $H_2O_2$ concentration-dependent, and the absorbance at 592 nm presents linear dependent with diversification of the concentration of $H_2O_2$ along with the formation of bromophenol blue. The linear data of absorbance dependence of $c(H_2O_2)$ was obtained by which we can be used to detect the $H_2O_2$.

In order to study on the function properties of vanadium (III) complexes, here, we synthesized two vanadium (III) complexes, $V(2,6\text{-pdc})_2(H_2O)_2\cdot 2H_2O$ (**1**), $V(2,6\text{-pdc})(htba)(H_2O)_2$ (**2**), ( 2,6-pdc = 2,6-pyridinedicarboxylic acid, htba = 2-acetoxy-4-trifluoromethylbenzoic acid ) and studied the bromination reaction activity and the detection of hydrogen peroxide.

## Experimental

### Materials and methods

Elemental analyses for C, H, and N were carried out on a Perkin Elmer 240C automatic analyzer. The infrared spectra were recorded on a JASCO FT/IR-480 spectrometer with pressed KBr pellets in the range 200-4000 $cm^{-1}$. UV-vis spectra were recorded on JASCO V-570 spectrometer (200-1500 nm, in form of solid sample). The X−ray powder diffraction data was collected on a Bruker AXS D8 Advance diffractometer using Cu–Kα radiation (λ = 1.5418 Å) in the 2θ range of 5–60° with a step size of 0.02° and a scanning rate of 3°/min.

### Synthesis of the Complexes

**$[V(2,6\text{-pdc})_2(H_2O)_2]\cdot 2H_2O$ (1)** $V_2(SO_4)_3$ (0.0390 g, 0.1 mmol),

2,6-pdc (0.0334 g, 0.2 mmol) and vitamin C (0.0180 g, 0.1mmol) were mixed and stirred for 3 h in a solution of $H_2O$ (15 mL) at room temperature forming a kind of yellow turbid solution (pH=6.5). Then, the mixture was sealed into a 23 mL Teflon-lined stainless steel autoclave and heated at 120℃. After 36 h, cooled to room temperature and yellow crystals suitable for X-ray diffraction were obtained. Yield (based on V): 0.0346g, 75.14%. Anal. Calc(%). For $C_{14}H_{15}N_2O_{12}V$: C, 36.94; H, 3.33; N, 12.31. Found: C, 36.91; H, 3.36; N, 12.30.

**V(2,6-pdc)(htba)($H_2O$)$_2$ (2)** $V_2(SO_4)_3$ (0.0390 g, 0.1 mmol), htba (0.0206 g, 0.1mmol), 2,6-pdc (0.0167 g, 0.1 mmol) and vitamin C (0.0180 g, 0.1mmol) were mixed and stirred for 2 h in a solution of $H_2O$ (15 mL) at room temperature forming yellow turbid solution (pH=6.5). The synthesized method of complex **2** was same as that of complex **1**. After 1 day, cooled to room temperature and yellow crystals of **2** was obtained. Yield (based on V): 0.0368 g, 80.49%. Anal. Calc(%). For $C_{15}H_9NO_9F_3V$: C, 39.37; H, 1.97; N, 3.06. Found: C, 39.38; H, 1.99; N, 3.05.

**X-ray Single crystal structural determinations**

Suitable single crystals of the two complexes were mounted on glass fibers for X-ray measurement, respectively. Reflection data were collected at room temperature with a Bruker AXS SMART APEX II CCD diffractometer (Bruker AXS, Karlsruhe, Germany) with graphite-monochromated Mo-Kα radiation (λ = 0.7107 Å) and a *ω* scan mode. All measured independent reflections (I > 2σ(I)) were used in the structural analysis and semi-empirical absorption corrections were applied using the SADABS program [32]. The structures were solved by the direct method using SHELXL-97[33]. The non-hydrogen atoms were refined with anisotropic thermal parameters. Hydrogen atoms of the organic frameworks were fixed at calculated positions with isotropic thermal parameters and refined using a riding model. Crystal data and structure refinements are shown in Table 1. The selected bond lengths and bond angles are listed in Table S1. Hydrogen bonds of the complexes **1**-**2** are given in Table S2.

**Measurement of bromination activity in solution**

Vanadium complex was dissolved in a mixed solution of 25 mL $H_2O$-DMF (DMF: 2 mL; $H_2O$: 23 mL). The reactions were initiated with the presence of phenol red solution ($10^{-4}$ mol·L$^{-1}$), buffer solution of $NaH_2PO_4$–$Na_2HPO_4$ (pH=5.8), KBr (0.4 mol·L$^{-1}$), vanadium complex (0.1 mmol·L$^{-1}$) and $H_2O_2$ (30%), and the bromination reaction activity tests were carried out at the constant temperature of 30±0.5 °C. The vanadium complexes with five different concentrations (measured 0.5mL, 1mL, 1.5mL, 2mL, 2.5mL respectively from 0.1 mmol·L$^{-1}$ vanadium complex) were placed in five cuvettes, and then put into the constant temperature water bath. The spectral changes were recorded using a UV1000 spectrophotometer at 592 nm and 5 min intervals, and the resulting data were collected during the reaction. The bromine reaction rate constant of vanadium complexes can be obtained according to the method of literature[30].

**Table 1** Crystallographic data and structure refinement for complexes **1**-**2***

| Complexes | **1** | **2** |
|---|---|---|
| Formula | $C_{14}H_{15}N_2O_{12}V$ | $C_{15}H_{11}NO_9F_3V$ |
| M (g mol$^{-1}$) | 454.22 | 457.19 |
| Crystal system | Triclinic | Monoclinic |
| Space group | *P*-1 | *P*2(1)/*c* |
| a (Å) | 8.540(2) | 15.3219(17) |
| b (Å) | 9.813(3) | 17.734(2) |
| c (Å) | 11.707(3) | 6.6947(8) |
| α (°) | 82.404(4) | 90 |
| β (°) | 73.547(4) | 90.641(2) |
| γ (°) | 68.028(4) | 90 |
| V (Å$^3$) | 872.2(4) | 1818.9(4) |
| Z | 2 | 4 |
| $D_{calc}$ (Mg m$^{-3}$) | 1.730 | 1.670 |
| Crystal size (mm) | 0.12*0.08*0.05 mm | 0.32*0.24*0.09 mm |
| F(000) | 464 | 920 |
| μ (Mo-Kα) / mm$^{-1}$ | 0.642 | 0.626 |
| θ (°) | 1.81 to 25.95 | 1.76 to 28.44 |
| Reflections collected | 4712 | 11358 |
| Independent reflections | 3313 | 4462 |

| ($I > 2\sigma(I)$) | | |
|---|---|---|
| Parameters | 262 | 312 |
| $\Delta(\rho)$ (e Å$^{-3}$) | 0.690 and -0.705 | 0.511and -0.467 |
| Goodness-of-fit | 1.044 | 1.037 |
| $R_1$[a] | 0.0555(0.0835)[b] | 0.0387(0.0567)[b] |
| $wR_2$[a] | 0.1371(0.1534)[b] | 0.0975(0.1066)[b] |

* [a] $R = \Sigma||Fo| - |Fc||/\Sigma|Fo|$, $wR_2 = [\Sigma(w(|Fo|^2-|Fc|^2)^2/[\Sigma(w(|Fo|^2)^2]^{1/2}$; $[|Fo|>4\alpha(|Fo|)]$.

[b] based on all data

## Results and discussion

### Synthesis discussion

Two vanadium (III) complexes have been successfully synthesized by the method of hydrothermal reaction at 120 °C (Scheme 1). Because the starting material $V_2(SO_4)_3$ (III) was not soluble in common solvents (methanol, ethanol, and water), forming a kind of yellow turbid solution in distilled water, so we used hydrothermal reaction, 120℃ to synthesize the complexes. In the synthetic process of the complexes, in order to prevent center metal vanadium (III) from being oxidized into vanadium (IV) or higher state, we tried various of reducing agents, such as KI, hydrazine hydrochloride, hydrazine hydrate and vitamin C to protect the center vanadium(III) to be oxidized. Finally, we found the vitamin C had the best effect for the synthesis, providing optimum pH (6.5) and reduction effect. Meanwhile, the temperature of the reaction could not too high, or the vanadium (III) atom might be oxidized into higher states. In addition, we found that the ethanoyl of triflusal was removed because of the acidic condition and hot-water backflow.

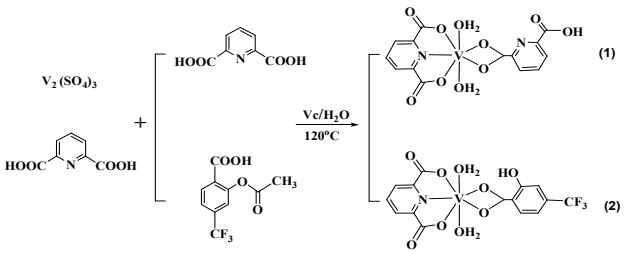


**Scheme 1:** The reaction process of the complexes **1** and **2**.

### IR spectra analysis

The IR spectra data of the complexes **1-2** (Fig. S1-S2) are listed in Table S3. It is clearly found that a broad absorption band appearing at 3417 and 3413 cm$^{-1}$ indicates the presence of water molecules. Absorption occurs in 3274, 3083, 2973 cm$^{-1}$ should be assigned to the stretching vibrations of C=C−H from pyrazolyl ring, benzene ring. The bands at 1623 for **1** and 1672 for **2** are attributed to the asymmetrical stretching vibration and symmetrical stretching vibration of C=O bond, respectively. For complex **1**, the peaks appear at 1433, 1395, 1209, 1182 and 1076 cm$^{-1}$ because of the stretching vibrations of pyrazolyl ring, and 1472, 1347, 1224, 1125 and 1060 in **2**. The bands at 934 and 875 for **1**, 925 and 878 cm$^{-1}$ for **2** are characteristic of the stretching vibrations of =C−CH. The bands at 746 and 679 for **1**, 753 and 684 cm$^{-1}$ for **2** are characteristic of the stretching vibrations of −C−H. The bands at 600 and 562 for **1**, 585 cm$^{-1}$ for **2** are characteristic of the stretching vibrations of V-$O_{water}$. The bands at 506 cm$^{-1}$ for **1** and 490 cm$^{-1}$ for **2** are attributed to the stretching vibration of V-$O_{carboxyl}$ respectively. Absorptions at 477, 457 are the characterization stretching vibration of V-N.

### UV-vis spectra analysis

The UV–vis spectra of complexes **1** and **2** (Fig. S3-S4) are recorded in the form of solid sample and their characteristic of the UV-vis bands are listed in Table S4. They have similar absorption patterns. Bands at 274 and 324nm for **1** and 274, 320 nm for **2** are attributed to the π-π* transition of the ligands. The band at 386 nm for **1** and 378 nm for **2** are assigned to LMCT (ligand to metal charge transfer) transition. The broad peak at 710 nm for **1** and 825 nm for **2** can be caused by the d→d* transition of the central metal vanadium.

### Structural description of complexes 1-2

**$[V(2,6\text{-pdc})_2(H_2O)_2]\cdot 2H_2O$ (1):** Structural analysis shows that complex **1** is crystallized in the triclinic system with *P*-1 space group. The molecular structure of **1** consists of a vanadium atom, two 2,6-pdc ligands, two coordinated water molecules and two free water molecules (Fig.1 ). The oxidation state of vanadium is +3. Vanadium atom displays a pentagonal bipyramid geometry, and it is coordinated by one nitrogen atom (N1) from 2,6-pdc ligand, four oxygen atoms (O1, O3, O5, O6 ) from 2,6-pdc ligands, two oxygen atoms (O9, O10) from coordinated water molecules. For two 2,6-pdc ligands, they adopt tridentate chelating coordination and bidentate coordination mode respectively, the bond length of V–N is 2.123(3)Å. For coordinated water molecules, they adopt terminal monodentate coordination, and the lengths of V–O is in the range of 2.056(3)-2.139(3)Å. The angles of the N-V-O is in the range of 72.99(12)-151.05(12)°. The angle of the O9-V-O10 is 177.10(11)°.

In addition, there are two kinds of inter-hydrogen bonds in the structure of the complex **1**, as illustrated in Table S2: (i) hydrogen bonds of O–H···O (O9–H9B···O1$^{\#1}$: 2.721(4)Å, 162.7°; O9–H9B···O5$^{\#1}$: 3.009(4)Å, 119.5°; O10–H10B···O3$^{\#1}$: 2.787(4)Å, 161.5; O10–H10B···O6$^{\#1}$: 3.016(4)Å, 124.9, #1: 1-x, -y, 1-z) are between the oxygen atoms (O1, O3, O5, O9) from 2,6-pdc ligands and the oxygen atoms (O9, O10) coordinated water. The molecules are connected to a 1D chain structure by these four hydrogen interactions (Fig.2 a). (ii) hydrogen bond of O–H···O(O10–H10A···O2$^{\#1}$: 2.802(4)Å, 141.9°) are between the oxygen atom (O2) from 2,6-pdc ligand and oxygen atom (O10) from coordinated water. Then, the neighbor chains are connected to a 2D sheet structure by hydrogen interactions of O10–H10A···O2$^{\#1}$ (Fig.2 b). (iii) hydrogen bonds of O–H···O(O9–

H9A···O2W$^{\#1}$: 2.724(4), 158.8°; O8–H8A···O2W$^{\#1}$: 3.240(5), 140.9°; O1W–H1WA···O8$^{\#1}$: 2.785(5), 133.9°; O1W–H1CW···O4$^{\#2}$: 2.780(5), 128.6°, #2=1-x, 1-y, 1-z) are between the oxygen atom from free water (O1W, O2W), coordinated water (O9) and 2,6-(pdc) ligands (O4, O8). Finally, the neighbor sheets are connected to a 3D network through four hydrogen interactions (Fig.2 c).

**V(2,6-pdc)(htba)(H2O)2 (2)** Complex **2** crystallizes in the monoclinic system with *P*2(1)/*c* space group. The molecular structure of **2** consists of one vanadium atom, one 2,6-pdc ligand, one htba ligand and two coordinated water molecules (Fig. 3). Vanadium atom may be best described as pentagonal bipyramid geometry, and it is coordinated by a nitrogen atom (N) and two oxygen atoms (O5, O7) from 2,6-pdc ligand, two oxygen atoms (O1, O2) from htba ligands, and two oxygen atoms (O1W, O2W) from coordinated water molecules. For 2,6-pdc ligand, it adopts tridentate chelating coordination mode and htba ligand adopts bidentate coordination mode. The bond length of V-N(1) is 2.1050(17) Å. For two coordinated water molecules, they adopt terminal monodentate coordination, the lengths of V-O is in the range of 2.0339(15) - 2.1201(16) Å. The angles of the N-V-O and O-V-O are in the range of 73.11(6) - 149.85(6)° and 61.21(6)- 178.69(7)°, respectively. The angle of the O1W-V-O2W is 178.69(7)°.

There are two kinds of hydrogen bonds in the structure of complex **2**. (i) the inter-hydrogen bonds of O–H···O (O1W–H1W···O4$^{\#1}$: 2.6224(19)Å, 175°; O2W–H2W···O6$^{\#2}$: 2.7187(19)Å, 169°; #1: 1-x, 1-y, 1-z; #2: x, 0.5-y, -0.5+z ) are between two oxygen atoms (O4, O6, O1W, O2W) from 2,6-pdc ligand and coordinated water molecule respectively. The hydrogen bonds O1W–H1W···O4$^{\#1}$ connect the molecules forming biopolymers structure (Fig.4 a), and the dipolymers further form a 2D sheet structure with the hydrogen bond O2W–H2W···O6$^{\#2}$ (Fig.4 b). (ii) intar-hydrogen bonds O–H···O (O3–H3A···O1: 2.588(3)Å, 148.3°) between two oxygen atoms from htba ligand, would be specified as S(6)[34], six atoms forming a closed six-membered ring.

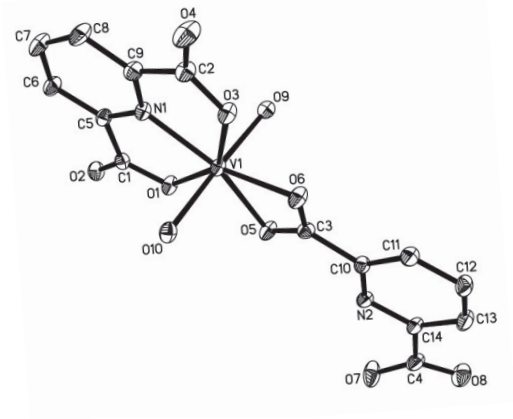


**Fig.1** : The molecular structure of **1.**

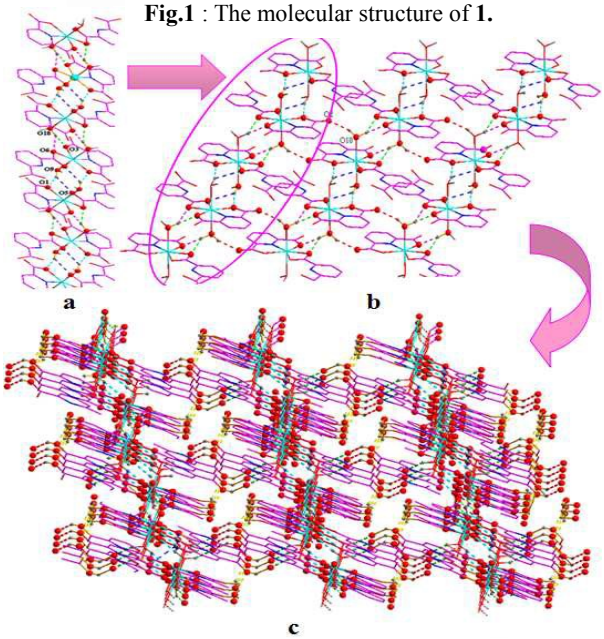


**Fig.2** a: 1D infinite chain structure of **1;** b: A view of a 2D supramolecular network structure formed by the hydrogen bonds;

**XRD analysis**

The powder X-ray diffraction data of the complexes **1** and **2** were obtained and compared with the corresponding simulated single-crystal diffraction data (Fig. S5-S6). The phase of the corresponding complex is considered as purities owning to the agreement of the peak positions. The different intensity may be due to the preferred orientation of the powder samples.

c: The 3D packing framework of the complex **1**.

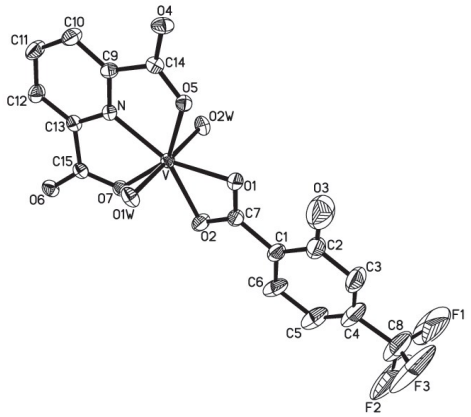


**Fig.3** : The molecular structure of **2**.

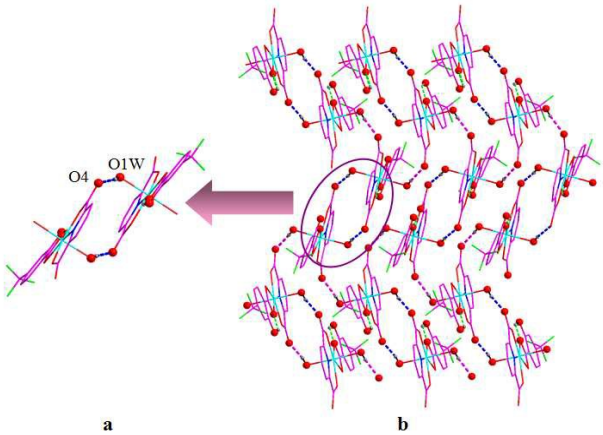


**Fig.4** a: The biopolymers structure of **2;** b:A view of a 2D supramolecular network structure formed by the hydrogen bonds.

**Mimicking catalytic bromination reaction**

To our knowledge, vanadium complexes are able of mimicking a reaction in which vanadium haloperoxidases catalyze the bromination of organic substrates in the presence of $H_2O_2$ and bromide. Herein, the catalytic bromination reaction activity of complexes **1** and **2** using phenol red as an organic substrate, which is shown by the conversion of phenol red to bromophenol blue have been investigated. The reaction is rapid (the maximum reaction rate constant was $2.424\times10^2$ k(mol $L^{-1})^{-2}s^{-1}$) and stoichiometric, producing the halogenated product by the reaction of oxidized halogen species with the organic substrate, and the reactive process is shown in Scheme 2.

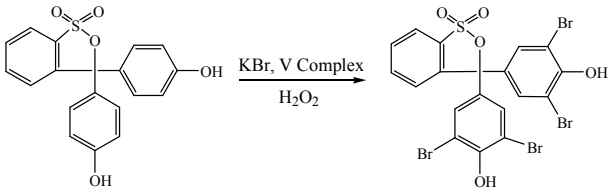


**Scheme 2:** Reactive process of the bromination reaction for the complexes.

The addition of solution of complex **1** to the standard reaction of bromide in a phosphate buffer with phenol red as a trap for oxidized bromine resulted in the visible color change of the solution from yellow to blue. The electronic absorption recorded a decrease in absorbance of the peak at 443 nm with the loss of phenol red and an increase of the peak at 592 nm with production of the bromophenol blue (shown in Fig. 5).

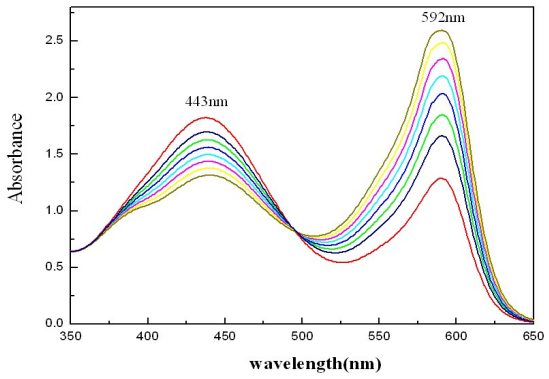


**Fig.5** Oxidative bromination of phenol red catalyzed by **1**. Spectral changed at 10 min intervals. The reaction mixture contained phosphate buffer (pH 5.8), KBr (0.4 mol·$L^{-1}$), phenol red ($10^{-4}$ mol·$L^{-1}$) $c_{(H2O2)}$=1 mol·$L^{-1}$ and complex **1** (0.1 mmol·$L^{-1}$).

Take complex **1** for an example to carry out kinetic studies of mimicking bromination reaction. A series of *dA/dt* data were obtained by changing the concentration of the vanadium complex, then the plot of -log (*dc/dt*) vs. -log*c* for complex **1** was depicted according to the data of Fig. 6, obtaining a straight line (Fig. 7) with a slope of 1.09 and an intercept of 2.0134. The former confirms the first-order reaction is dependent on vanadium. Based on the equation of "$b=log\ k + ylog\ c_2 + zlog\ c_3$", the reaction rate constant, k, is determined by the concentrations of KBr and phenol red ($c_2$ and $c_3$), the reaction orders of KBr and phenol red (*y* and *z*), as well as *b*. While in the experiment, considering that the reaction orders of KBr and phenol red (*y* and *z*) are 1 according to the literature; $c_2$ and $c_3$ are known to be 0.4 mol/L and $10^{-4}$ mol/L, respectively, so the reaction rate constant (*k*) for complex **1** can be calculated as $2.424\times10^2$ $(mol/L)^{-2}$ $s^{-1}$. Similar plots for **2** was generated in the same way (Fig. 8, Fig. 9 ), and values of the slope and the intercept is 1.0048, 2.2403.

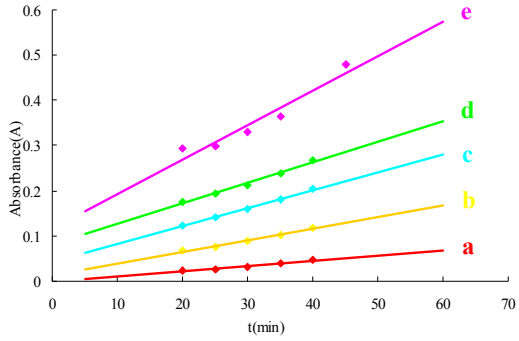


**Fig.6**. A series of linear calibration plots of the absorbance at 592 nm dependence of time for different concentration of the complex **1**. Condition used: pH=5.8, c(KBr)=0.4 mol·$L^{-1}$, $c(H_2O_2)$=1 mol·$L^{-1}$, c(phenol red)=$10^{-4}$ mol·$L^{-1}$. c(complex 0.1/mmol·$L^{-1}$)= a: $1.2\times10^{-3}$; b: $2.6\times10^{-3}$; c: $4\times10^{-3}$; d: $4.5\times10^{-3}$ ; e: $7.6\times10^{-3}$.

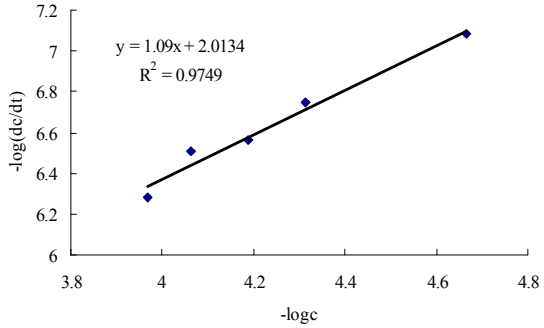


**Fig.7** –log (dc/dt) dependence of –logc for **1** in DMF-$H_2O$ at 30±0.5°C

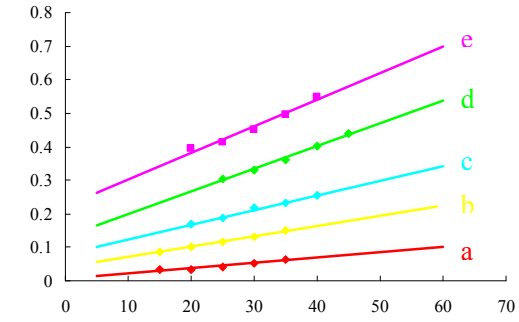


**Fig.8** A series of linear calibration plots of the absorbance at 592 nm dependence of time for different concentration of the complex **2**. Condition used: pH=5.8, c(KBr)=0.4 mol·$L^{-1}$, $c(H_2O_2)$=1 mol·$L^{-1}$, c(phenol red)=$10^{-4}$ mol·$L^{-1}$. c(complex 0.1/mmol·$L^{-1}$)= a: $1.6\times10^{-3}$; b: $3.1\times10^{-3}$; c: $4.4\times10^{-3}$; d: $6.7\times10^{-3}$ ; e: $7.9\times10^{-3}$.

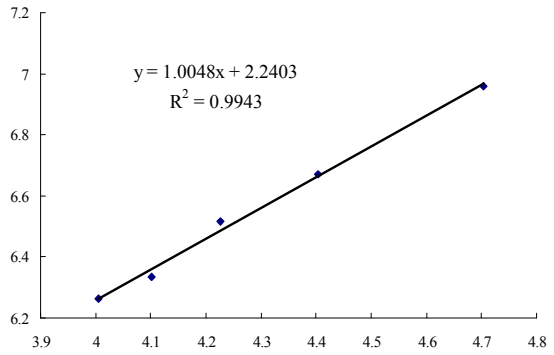


**Fig 9.** –log (dc/dt) dependence of –logc for **2** in DMF-$H_2O$ at 30±0.5°C

The cyclic catalytic brominated reaction mechanism was shown in Scheme 3. Two complexes were coordinated by two water molecular as they were shown in a ($[V(H_2O)_2L_1L_2]$). The vanadium complex was easily to lose a $H_2O$ forming a compound b ($[V(O_2)L_1L_2H_2O]$) with $H_2O_2$ as an oxidation regent. The formation process of c ($[VO_2L_1L_2]$) was same with b. c was oxidized to form an intermediate compound d ($[V(O_2)L_1L_2H_2O]$). $Br^-$ was oxidized rapidly by d, while at the same time HOBr and c were formed with the lossing of $OH^-$. The following process was similar to previous reaction, and the other coordinated water was oxidized with $H_2O_2$ forming an intermediate d. Vanadium haloperoxidases model c oxidized $Br^-$ into HOBr which further brominated oxidized phenol red. c and d cycle reaction continued until the phenol red transformed into bromophenol blue completely.

**Scheme 3:** The cyclic catalytic bromination reaction mechanism

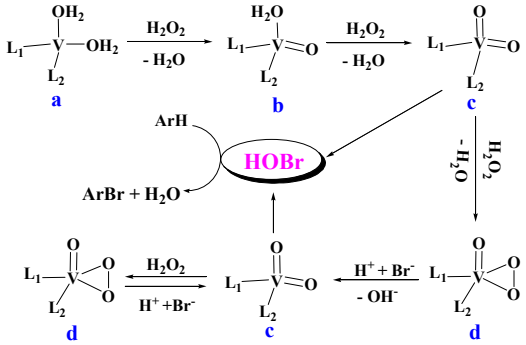


The experiment results showed that: (i) the reaction orders of the vanadium complexes in the bromination reaction are all close to 1, confirming appreciatively the first-order dependence on vanadium; (ii) the reaction rate constants of the two complexes is **1>2**( Table 2).

**Table2** Kinetic data for the complexes in DMF–$H_2O$ at 30±0.5 °C

| Complexes | m | b | k(mol $L^{-1}$)$^{-2}s^{-1}$ |
|---|---|---|---|
| **1** | 1.09 | 2.0134 | $2.424\times10^2$ |
| **2** | 1.00 | 2.2403 | $1.437\times10^2$ |

Conditions used: c(phosphate buffer) = 50 mmol·$L^{-1}$, pH = 5.8, c(KBr) = 0.4 mol·$L^{-1}$, c(phenol red) = $10^{-4}$mol·$L^{-1}$.“*x*” is the reaction order of the vanadium complex; “*b*” is the intercept of the line; “*k*” is the reaction rate constant for the vanadium complex.

Analysis results found that vanadium (III) complexes showed slightly different but high catalytic activity. The order of the reaction rate constant for complexes is **1**>**2**. We thought the catalytic reaction rate was influenced by the forming of intermediate species. In complex **1**, bonds length of V-O between center metal vanadium and coordinated water were 2.076, 2.070, while 2.056, 3.034 in **2**. We knew that the longer of the bonds were, the weaker of the bond energy was. Hence, the V-O bonds in **1** were easier to break to form an intermediate species than **2**, so the reaction rate of **1** was faster than that of **2**. On the other hand, there was a same ligand (2,6-pdc) and same coordinated model in the complexes, but the only difference in the structure was the other ligand, 2,6-pdc for **1**, htba for **2**. The space steric effect of htba was bigger than that of 2,6-pdc, because there was a vicinal hydroxyl on the benzene of htba. Therefore, the coordinated $H_2O$ was easier to be oxidized to form an intermediate species. So the reaction rate constant was **1**>**2**.

## Colorimetric Detection of Hydrogen peroxide

As we can see, hydrogen peroxide play an important role in food, clinical physic, pharmaceutical production and environment protection fields, especially it has great practical effect in catalytic reaction. Based on the view, we studied the effect of the concentration of $H_2O_2$ upon our catalytic reaction to furthermore extend a new $H_2O_2$ detection method. Through the experiment results, it was found that the oxidation reaction catalyzed by the vanadium complexes is $H_2O_2$ concentration-dependent, and the absorbance at 592 nm presents line relativity with diversification of the concentration of $H_2O_2$ along with the formation of bromophenol blue in 25 min. The linear data of absorbance dependence of c($H_2O_2$) was obtained (Fig.10, Fig.11). And the detection limit value of the concentration $H_2O_2$ was estimated to be 0.94 mol/L for **1**, 0.98 mol/L for **2** by stretching of the line. All these observations further confirmed that the catalytic reaction system can be used as a potential method for the detection of $H_2O_2$.

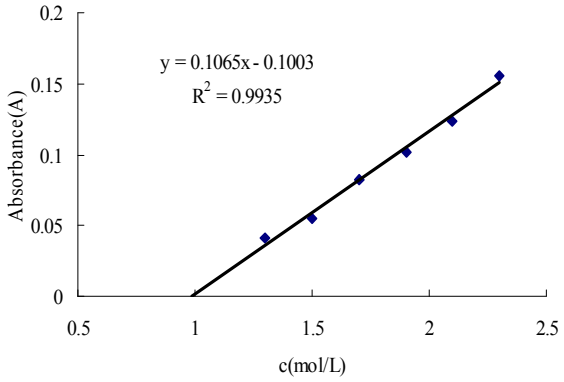


**Fig.10** The linear calibration plot of the absorbance at 592 nm on the concentration of $H_2O_2$ from complex **1** as catalyzer in DMF–$H_2O$ at 30 ± 0.5 °C.

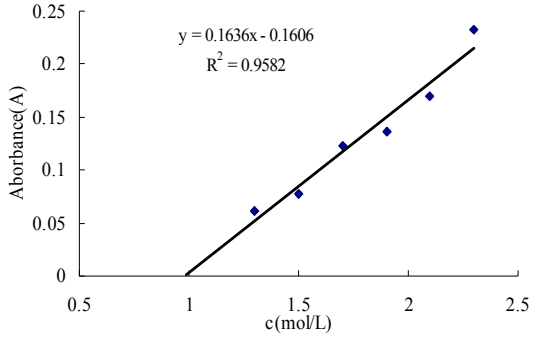


**Fig.11** The linear calibration plot of the absorbance at 592 nm on the concentration of $H_2O_2$ from complex **2** as catalyzer in DMF–$H_2O$ at 30 ± 0.5 °C.

Furthermore, comparisons of the detection limit for the complexes reported previously are listed in Table 3. Complexes **3** and **4** were synthesized according to their corresponding reference[30]. **3** is an oxidovanadium (IV) complex with a V=O bond coordinated by a 1, 10-phenanthroline and an oxalic acid ligand. **4** is also an oxidovanadium (V) complexe with two V=O bonds coordinated by a bpz*T-O ligand (bpz*T-O: 4,6-bis(3,5-dimethylpyrazol-1-yl)-1,3,5-triazin-2-olate). The order of the reaction rate constant for them is **4**>**3**>**2**>**1**. It is found that the **1** and **2** have similar detection limit, which is related to the structure of the complexes. The increasing valence of the vanadium would reduce the selectivity of hydrogen peroxide. Moreover, the coordinated mode also has effect on the detection limit, for more coordination number would impede the process of the reaction.

**Table 3:** The detection limit for the complexes

| Complexes | LOD( mol/L ) |
|---|---|
| **1** | 0.94 |
| **2** | 0.98 |
| **3** | 1.10 |
| **4** | 1.19 |

## Conclusions

Two new vanadium (III) complexes were successfully synthesized firstly. Structure analysis showed that they have similar coordinated environment and the vanadium (III) atoms were seven-coordinated with a NO6 donor set in a pentagonal bipyramid geometry. We tested the bromination reaction activities and finally found the reaction rate constants (k) of complexes **1** and **2**, which indicated that they can be considered as potential functional models of vanadium haloperoxidases. Furthermore, a new colorimetric detection method based on the catalytic bromination reaction for the detection of $H_2O_2$ have been discovered, this detection system was simple and sensitive. We will deeply investigate the application of the detection reaction mechanism in the future.

## Supplementary material

Tables of atomic coordinates, isotropic thermal parameters, and complete bond distances and angles have been deposited with the Cambridge Crystallographic Data Center. Copies of this information may be obtained free of charge, by quoting the publication citation and deposition numbers CCDC 1056936 (**1**), 1056937 (**2**), from the Director, CCDC, 12 Union Road. Cambridge, CB2 1EZ, UK (Fax+44-1223-336033; e-mail deposit@ccdc.cam.ac.uk; http://www.ccdc.cam.ac.uk

## Acknowledgements

This work was supported by the grants of the National Natural Science Foundation of China (Grant No. 21071071, 21371086), and Commonweal Research Foundation of Liaoning province in China (No.2014003019) for financial assistance.

## Notes and references

[a] *College of Chemistry and Chemical engineering, Liaoning Normal University, Huanghe Road 850#, Dalian City, 116029, P.R. China. tel: 0411-82156987; E-mail: xingyongheng2000@163.com*
[b] *College of Life Science, Liaoning Normal University, Dalian 11602, P.R. China*

1. Y. Zuo, J. Hoigné, *Science*, 1992, **260**, 71.
2. A. Tahirovic, A. Copra, E. Omanovic-Miklicanin and K. Kalcher, *Talanta*, 2007, **72**, 1378.
3. (a) E. Linley, S. P. Denyer, G. McDonnell, C. Simons, and J. Y. Maillard**,** *J. Antimicrob. Chemother*, 2012, **67**, 1589; (b) W. Chen, S. Cai, Q.-Q. Ren, W. Wen and Y.-D. Zhao, *Analyst*, 2012, **137**, 49; (c) T. P. Fellinger, F. Hasché, P. Strasser and M. Antonietti, *J. Am. Chem. Soc.*, 2012, **134**, 4072.
4. (a) Z. M. Pei, Y. Murata, G. Benning, S. Thomine, B. Klüsener, J. G. Allen, E. Grill and J. I. Schroeder. *Nature*, 2000, **406**, 731; (b) Y. Xiao, H.-X. Ju and H.-Y. Chen, *Anal. Chim. Acta.*, 1999, **391**, 73; (c) T. Matoba, H. Shimokawa, M. Nakashima, Y. Hirakawa, Y. Mukai, K. Hirano, H. Kanaide and A. Takeshita, *J. Clin. Invest.*, 2000, **106**, 1521.
5. (a) K. S waminathan, S. Sandhya, A. C. Sophia, K. Pachhade and Y. V. Subrahmanyam, *Chemosphere*, 2003, **50**, 619; (b) H. N. Kim, M. H. Lee, H. J. Kim, J. S. Kim and J. Yoon, *Chem. Soc. Rev.*, 2008, **37**, 1465.
6. J. Wang, Y. Lin and L. Chen, *Analyst*, 1993, **118**, 277.
7. (a) P. Niethammer, C. Grabher, A. T. Look and T. Mitchison, *Nature*, 2009, **459**, 996; (b) F. Sauer, S. Limbach and G. K. Moortgat, *Atmos. Environ.*, 1997, **31**, 1173; (c) M. M. Tarpey, I. Fridovich, *Circ. Res.*, 2001, **89**, 224,
8. (a) J. Tang, B. Wang, Z. Wu, X. Han, S. Dong and E. Wang, *Biosens. Bioelectron.*, 2003, **18**, 867; (b) A. A. Karyakin, E. E. Karyakina and L. Gorton, *Anal. Chem.*, 2000, **72**, 1720; (c) B. C. Dickinson, C. J. Chang, *J. Am. Chem. Soc.*, 2008, **130**, 9638.
9. (a) C. Matsubara, K. Kudo, T. Kawashita and K. Takamura, *Anal. Chem.*, 1985, **57**, 1107; (b) M. C. Y. Chang, A. Pralle, E. Y. Isacoff and C. J. Chang, *J. Am. Chem. Soc.*, 2004, **126**, 15392; (c) E. A. Veal, A. M. Day and B. A. Morgan, *Mol. Cell*, 2007, **26**, 1.
10. S. P. Wolff, *Methods Enzymol.*, 1994, **233**, 182.
11. P. A. Tanner and A. Y. S. Wong, *Anal. Chim. Acta*, 1998, **370**, 279.
12. W. Luo, M. E. Abbas, L. Zhu, K. Deng and H. Tang, *Anal. Chim. Acta*, 2008, **629**, 1.
13. E. W. Miller, O. Tulyanthan, E. Y. Isacoff and C. J. Chang, *Nat. Chem. Biol.*, 2007, **3**, 263.
14. M. J. Navas, A. M. Jimenez and G. Galan, *Atmos. Environ.*, 1999, **33**, 2279.
15. G. De. Faveri, G. Ilyashenko and M. Watkinson, *Chem. Soc. Rev.*, 2011, **40**, 1722.
16. M. Abo, Y. Urano, K. Hanaoka, T. Terai, T. Komatsu and T. Nagano, *J. Am. Chem. Soc.*, 2011, **133**, 10629.
17. (a) S. Qian, Y. Chen, L. J. Deterding, Y. C. Fann, C. F. Chignell, K. B. Tomer and R. P. Mason, *Biochem. J*, 2002, **363**, 281; (b) D. H.

Bremner, A. E. Burgess, D. Houllemare and K. C. Namkung, *Appl. Catal. B: Environ.*, 2006, **63**, 15; (c) A. H. Vetter, A. Berkessel, *Tetrahedron lett.*, 1998, **39**, 1741.

18. (a) S. Woo, Y. R. Kim, T. D. Chung, Y. Piao and H. Kim, *Electrochim. Acta*, 2012, **59**, 509; (b) K. J. Huang, D. J. Niu, X. Liu, Z. W. Wu, Y. Fan, Y. F. Chang and Y. Y. Wu, *Electrochim. Acta*, 2011, **56**, 2947; (c) M. Liu, R. Liu and W. Chen, *Biosens. Bioelectron.*, 2013, **45**, 206.
19. (a) W. Chen, L. Hong and A.-L. Liu, *Talanta,* 2012, **99**, 643; (b) Y. B. Tsaplev, *J. Anal. Chem.*, 2012, **67**, 506; (c) W. Shi, X. Zhang, S. He and Y. Huang, *Chem. Commun.*, 2011, **47**, 10785.
20. C. Paul, G. Pohnert, *Nat. Prod. Rep.*, 2011, **28**, 186.
21. (a) M. Isupov, A. Dalby, A. Brindley, T. Izumi, T. Tanabe and J. Littlechild, *J. Mol. Biol.*, 2000, **299**, 1035; (b) J. Littlechild, E. Garcia-Rodriguez, *Coord. Chem. Rev.*, 2003, **237**, 65.
22. M. Almeida, S. Filipe, M. Humanes, M. F. Maia, R. Melo, N. Severino, J. A. L. da. Silva, J. J .R. Fraústo da Silva and R. Wever, *Phytochemistry*, 2001, **57**, 633;
23. R. Ullrich, J. Nüske, K. Scheibner, J. Spantzel and M. Hofrichter, *Appl. Environ. Microbiol.*, 2004, **70**, 4575;
24. (a) A. Butler, *Coord. Chem. Rev.*, 1999, **187**, 17; (b) G. R. Nosrati, K. N. Houk, *Biochem.*, 2012, **51**, 7321; (c) M. Sandy, J. N. Carter-Franklin, J. D. Martin and A. Butler, *Chem. Commun.*, 2011, **47**, 12086.
25. (a) F. Natalio, R. André, A. F. Hartog, B. Stoll, K. P. Jochun, R. Wever and W. Tremel, *Nat. Nanotech.*, 2012, **7**, 530; (b) G. E. M. Winter, A. Butler, *Biochem.*, 1996, **35**, 11805;
26. (a) Y.-H. Xing, K. Aoki, F.-Y. Bai, Y.-H. Zhang and B.-L. Zhang, *J. Chem. Crystallogr.*, 2008, **38**, 327; (b) N. Teshima, M. Kuno, M. Ueda, H. Ueda, S. Ohno and T. Sakai, *Talanta*, 2009, **79**, 517.
27. Y.-Z Cao, H.-Y. Zhao, F.-Y. Bai, Y.-H. Xing, D.-M. Wei, S.-Y. Niu and Z. Shi, *Inorg. Chim. Acta*, 2011, **368**, 223.
28. H.-Y. Zhao, Y.-H. Xing, Y.-Z. Cao, Z.-P. Li, D.-M. Wei, X.-Q. Zeng and M.-F. Ge, *J. Mol. Struct.*, 2009, **938**, 54.
29. H.-Y. Zhao, Y.-H. Zhang, Y.-H. Xing, Z.-P. Li, Y.-Z. Cao, M.-F. Ge, X.-Q. Zeng and S.-Y. Niu, *Inorg. Chim. Acta*, 2009, **362**, 4110.
30. C. Chen, Q. Sun, D.-X. Ren, R. Zhang, F.-Y. Bai and Z. Shi, *Cryst. Eng. Commun.*, 2013, **15**, 5561.
31. D.-X. Ren, N. Xing, H. Shan, C. Chen, Y.-Z. Cao and Y.-H. Xing, *Dalton Trans*, 2013, **42**, 5379.
32. G. M. Sheldrick, SADABS, *Program for Empirical Absorption Correction for Area Detector Data*, University of Götingen, Götingen, Germany, **1996**
33. G. M. Sheldrick, SHELX-97, *Program for Crystal Structure Analysis,* University of Gottingen: Gottingen, Germany, **1997**
34. J. Bernstein, R. E. Davis, L. Shimoni and N. L. Chang, *Angew. Chem. Int. Ed.,* 1995, **34**, 1555.

For Table of Contents Use only

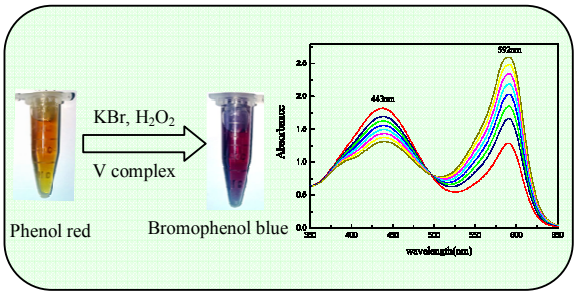


Text:

Two vanadium(III) complexes were synthesized. Hydrogen peroxide was detected by colorimetric method of catalytic bromination reaction with complexes as catalyst.